



J. Serb. Chem. Soc. 86 (3) 299–311 (2021)
JSCS–5422

Electrochemical formation of ion-conducting oxo-phosphate-molybdate polymer on aluminium

HUSSEIN HUSSEIN^{1*}, SWETLANA POPOVA², IRINA FROLOVA²
and MARINA LOPUKHOVA²

¹Department of Chemistry and Chemical Technology of Materials, Yuri Gagarin State
Technical University of Saratov, Saratov, Russia and ²Engels Technological Institute (branch)
of Yu. Gagarin Saratov State Technical University, Engels, Russia

(Received 13 September, revised 27 November, accepted 8 December 2020)

Abstract: The state of the electrochemical behaviour of the Al electrode in aqueous solutions containing $\text{Na}_2\text{MoO}_4 + \text{H}_3\text{PO}_4 + \text{chitosan}$ was investigated by methods of currentless chronopotentiometry, chronoamperometry, optical and scanning electron microscopy. The modification of the surface polymolybdate phosphate layers was carried out in a potentiostatic mode in the potentials range from -1 to -3 V and polarization time (from 15 to 90 min). The elemental composition of the surface layer of the metal before and after cathodic polarization were investigated. The electrochemical formation of matrix polymeric structures from ion-conducting (H^+ , Na^+) heteronuclear polymolybdate and polyphosphate-molybdate complexes of double salts $\text{Na}_6\text{Al}_n\text{Mo}_{7-n}\text{O}_{24}$ and $\text{Na}_{2y}\text{Al}_2(\text{MoO}_4)_y(\text{PO}_4)_{3-y}$ was established. The rate of hydrogen and sodium intercalation into the structure of the polyoxophosphate-molybdate layer increased sharply with an increase of the potential range from -1.3 to -3.0 V. The addition of chitosan into the solution enhances the film-forming effect of surface ion-conducting oxo-phosphate – molybdate polymeric layer.

Keywords: energy carrier; hydrogen sorption; polymolybdate phosphate; aluminium hydrides; hydrogen; chronopotentiometry.

INTRODUCTION

The problem of hydrogen storage has remained in the focus of scientific research for many decades.^{1,2} Hydrogen is the most abundant element in the universe, it has the highest energy density per unit mass. Being an energy carrier, mainly derived from water, hydrogen turns back into water when burned. This ensures the ecological safety of hydrogen production for the environment, its energy and economic competitiveness. In this regard, electrochemical methods^{3,4} of hydrogen production can be very effective. Therefore, research on the problem

* Corresponding author. E-mail: hussein-2010@mail.ru
<https://doi.org/10.2298/JSC20913081H>

of developing an electrochemical technology for generating hydrogen and its accumulation and storage is urgent and requires the search and study of the properties of hydride-forming metals and alloys, as well as methods for controlling the kinetics of hydrogen sorption and the sorption capacity of the hydrogen-sorbing material.⁵⁻⁷ A directed effect on the surface and bulk properties of the sorbing material, on the concentration of structural defects and the hydrogen sorption capacity can be made by the electrochemical modification using the method of cathode incorporation.^{5,6,8,9}

Recently, scientists and technologists have shown particular interest in aluminum,¹⁰⁻¹⁵ due to its low specific gravity, non-toxicity, high purity of hydrogen generated by the reaction of aluminum with water, the ease of formation and the ability to use commercial aluminum alloys. It is also important that the alkali formed during the reaction acts as a catalyst and it can be completely recovered, and finally, the used devices can be recycled.

The standard electrode potential of aluminum is -1.676 V. Aluminum is a reactive metal with a high affinity for oxygen.¹⁶ The strongest activators of aluminum⁷ in the alkaline medium are OH ions. The thickness of the formed oxide layers can vary from 50 to 100 Å. The presence of pores facilitates the occurrence of chemical and electrochemical reactions and the localization of products in the pores of the oxide layer.^{16,17} The dependence of the stationary potential Al on the pH medium in acidic solutions from 1 to ~6 is described by the equation: $E_{\text{stat}} = -0.26 - 0.063\text{pH}$. The corrosion resistance of Al under atmospheric conditions is explained by the presence of a natural film of Al_2O_3 or $\text{Al}_2\text{O}_3 \times \text{H}_2\text{O}$ on its surface with a thickness from 0.005 to 0.015 μm . The electrochemical modification allows to vary the composition of the oxide film, its structure and properties.^{8,9,11,15,17}

The activation of the surface oxide layer by the modification with the atoms of other elements is accompanied by the separation of the aluminum-oxygen layers and the formation of a spinel-type structure, in which aluminum ions in tetrahedral spaces are replaced by ions of the incorporated metal.^{8,9,17,18}

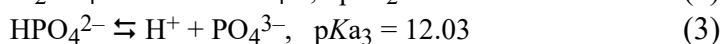
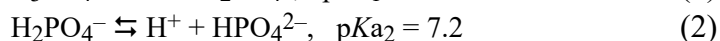
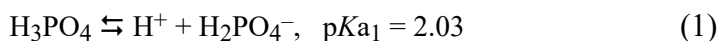
Studies show that the main factor determining the properties of aluminum oxide, if we imagine its composition in the form of a hydroxo-anionic complex $n(\text{Al}_2\text{O}_3-x)m(\text{An}^{z-})p(\text{OH}^-)q(\text{H}_2\text{O})$ is the nature of the electrolyte.^{5,6,8,11,16} The channel (tunnel) structure should facilitate the sorption or incorporation of particles of various substances. In this case, the nature of the anion in the electrolyte solution has a significant effect on the adhesion of the reaction product with the metal surface.^{5,8,15}

In the group of hydroxy acids, the adhesion turned out to be the highest in phosphoric acid due to the largest pore diameter in the formed oxide layer, mainly because of the occurrence of chemical bonds between the incorporated particles and structural elements of the aluminum oxide.^{6,17,19}

Due to the distorted tetrahedral shape of the structural cell, the phosphates have a high deformation and polarization ability and, accordingly, a high degree of chemical adhesion on the aluminum oxide. The increase in the electrical conductivity of such a modified oxide layer, by alloying with a third component, can be explained by the following factors:^{15,16}

- higher transport properties of the modified layer (Na₂O, Al₄O₃) due to the disappearance of anisotropy and disordering of the cation sublattice;
- the formation of cation vacancies V_C ;
- the increase in the size of migration channels.

If we take into account, the dependence of the dissociation reaction of phosphoric acid on pKa the results are as follows:



then H_2PO_4^- should possess the highest adsorption, presumably because of the formation of a chemical bond of the O–M type with the surface metal atoms of the electrode. A slight increase in the adsorption of H_2PO_4^- , observed during the cathodic polarization, can be explained by their reorientation by hydrogen atoms to the metal surface: $(\text{HO})_2\text{PO}_2^-$. Thus, polar anions of the H_2PO_4^- type can be adsorbed either through hydrogen atoms or through oxygen atoms.

If cathodic polarization is applied to the metal being treated, the discharge of H^+ and, accordingly, the growth of pH of the near-electrode layer will significantly accelerate, providing the formation of a precipitate of hardly soluble phosphates, for example, during cathodic polarization in a phosphating solution.^{20–22} The stretching vibration of the P–OH group detected by IR spectroscopy at a frequency of $\nu = 1010 \text{ cm}^{-1}$ indicates the presence of a substance with the composition $\text{Al}_2(\text{HPO}_4)_3$ in the surface layer. Metals (aluminum, titanium) behave similarly during the cathodic polarization in solutions containing phosphoric acid (or its soluble salts) and the additives of molybdates, tungstates of alkali metals.^{18,20–23}

In this regard, inorganic compounds are of interest, the porous structure of which are based on a tetrahedral phosphate framework capable of trapping cations in their cavities. The transfer of cations along the channels of such structures at a high rate is possible, provided that the width of the narrowest point in the crystallographic channel is greater than the doubled sum of the radii of the mobile cation and oxygen. Moreover, the cationic conductivity can be significantly increased by varying the lattice parameters due to the heterovalent substitutions in the sublattices of both the alkali metal and phosphorus. With the addition of the Mo^{6+} into the phosphorus sublattice, the electrical conductivity increases, and the higher is the Mo^{6+} content, the greater is conductivity.¹⁶ An

increase in ionic conductivity in solid solutions Me_xPO_4 ($\text{Me} = \text{Na}$ to Cs) at heterovalent substitutions is explained by the formation of vacancies in the alkali metal sublattice associated with the solubility of the additive. Besides, the size of the modifying cation cannot be neglected.¹⁸

It is also possible to improve the conductivity by creating compositions with a flexible structure that can withstands a wide range of substitutions in cationic and anionic groups, with the formation of substitutional solid solutions containing a large number of mobile cations, including multiply charged ones.^{18,19} In the case of heterovalent substitution of, for example, a part of phosphorus (V) by silicon (IV), a deficiency of positive charge occurs, which is compensated by the incorporation of an additional amount of Na^+ , which are statistically distributed over 18-fold positions, which leads to high ionic conductivity.^{16,18}

Thus, the presence of ionic conductivity in phosphates allows us to expect that the formation of a phosphate-containing coating on aluminum should not prevent reversible intercalation-deintercalation of alkali and alkaline-earth metal ions.^{13,15} Moreover, due to various iso- and heterovalent substitutions in the sublattice of the structure-forming element (Al) and phosphorus, due to its inevitable deformation, it becomes possible to obtain materials with the desired functional properties. In this regard, it seems relevant to study the effect of the elemental composition of the polymeric multinuclear phosphate-containing oxide of the molybdate coating, formed by heterovalent substitution under cathodic polarization on the capacitive characteristics of the Al electrode, when an organic polymer with a high film-forming effect, biopolymer chitosan, is added into the electrolyte composition.

Due to the ability to form non-covalent complexes with other polyelectrolytes, high sorption activity with ions of various metals, the ability to retain both the solvent and substances dissolved in its structure, chitosan is one of the promising research objects that have found application in various branches of science and technology, biotechnology and medicine. Of particular interest is its ability to form fibers and films. Chitosan films favourably differ in their strength, elasticity, uniformity in thickness, and transparency.²³⁻²⁷

When modified, in particular, with phosphoric acid, the ability of chitosan to form fibers and films increases, as well as its sorption properties.²⁴⁻²⁸ Phosphoric acid, as a strong nucleophile (reagent), can affect the position of OH groups connected with the terminal glycosidic center of the chitosan molecule. Probably, the phosphoric acid anion can form a stable complex with the terminal glycosidic center of chitosan. In this complex, the position of the OH group is fixed in the configuration that makes the greatest contribution to the specific rotation (Fig. 1).

The study of the effect of chitosan on the electrochemical behaviour of polyphosphate molybdate complexes on metal electrodes through the stage of the

formation of polyelectrolyte complexes in the solution and their subsequent adsorption on the electrode is a promising direction²⁹ in electrochemistry of heteronuclear polyelectrolyte structures, which determines the kinetics of cathodic incorporation of alkali metals and hydrogen into the electrode metal by the mechanism of intercalation – deintercalation.

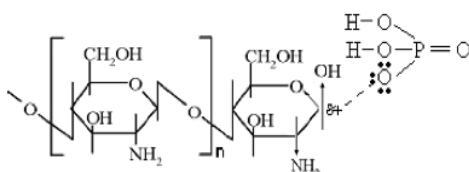


Fig. 1. Formation of a complex of chitosan with phosphoric acid.

EXPERIMENTAL

The method of the preparation of the working solution included the following operations: chitosan (previously ground) was completely dissolved in phosphoric acid at 40 ± 0.5 °C.²⁷ The temperature was maintained using a U-15 laboratory recording thermostat. A thin stream of phosphoric acid with chitosan dissolved in it was added and thoroughly mixed until homogeneous in a flask half filled with distilled water. Then sodium molybdate was dissolved in a small amount of water, thoroughly mixed and added into a volumetric flask.

For the electrochemical treatment of the system $\text{Al}/\text{Na}_2\text{MoO}_4$ (0.01 M) + H_3PO_4 (1 M) + chitosan (4 g/l), the solutions were prepared in volumetric flasks 1000 ml: $\text{Na}_2\text{MoO}_4 \cdot 2\text{H}_2\text{O}$ (2.42 g), H_3PO_4 (57.65 g) and chitosan (4 g). It was carried out using a potentiostat-galvanostat P-8S (LLC “Elins”), combined with a computer and equipped with a program developed by the manufacturer. The potential of the chloride silver electrode in the test solutions was measured and expressed relative to a standard silver chloride reference electrode ($C_{\text{Cl}} = 1$ M, at $t = 25$ °C, $E^0_{\text{Cl}^-/\text{AgCl}/\text{Ag}} = 0.222$ V). Besides the effect of the potential and the duration of electrolysis, the effect of the degree of chitosan dispersion was investigated by varying the grinding time of chitosan flakes within 30 to 60 min, using a Philips electric mill.^{24,27} The surface of the modified electrodes was investigated using the methods of current-free chronopotentiometry, optical microscopy²⁹ in the direct and reflected light^{30,31} (microscope MINIMED 5021 and Axio Ymager A2m, manufactured by ZEISS, Germany). The elemental composition of the surface layer of modified electrodes was determined by scanning electron microscopy.^{30–32} All studies were carried out at the temperature of 20 ± 2 °C. Each experiment was repeated 3 times and the average statistical value of the fixed current (or potential) value was determined.³³

The objects under study were aluminum foil plates Al: 97.5 % (impurities P 1.52 %, Mn: 0.56 %, Fe: 0.42 %), which were preliminarily subjected to degreasing with ethanol and mechanical polishing with sandpaper (or glass powder of double decantation).³⁴ Reagents used in the work were $\text{Na}_2\text{MoO}_4 \cdot 2\text{H}_2\text{O}$ of grade “h” GOST 10931-71, H_3PO_4 of grade “chda” GOST 6552-80, flake chitosan produced by OOO “Chitosan Technologies” (Engels, Saratov region) with molecular weight 120 kDa, size of flakes 0.1 to 3.0 mm. All solutions were prepared in bidistilled water.

The modification of the surface polymolybdate phosphate layers²⁹ was carried out in a potentiostatic mode in the range of potentials from -1 to -3 V and at different polarization time (15 to 90 min). The electrodes were immersed in the studied solutions of

$\text{Na}_2\text{MoO}_4 \cdot 2\text{H}_2\text{O}$ (0.01 mol/l) and the mixtures with H_3PO_4 (1 mol/l) without and with the addition of chitosan (4 g/l), the dispersed time was 30, 40 and 60 min, the molecular weight 250. Electrochemical treatment was carried out using Elins R-301 potentiostat-galvanostat (manufactured by Elins LLC), combined with a computer and equipped with a program developed by the manufacturer, which allowed to convert the digital record into graphic dependences to determine the polarization characteristics (current-free potential E , current density and polarization time under the specified experimental conditions). The current-free potential was recorded for 300 s before and after cathodic polarization in a solution of a given composition, until a stationary value did not change over time.

RESULTS AND DISCUSSION

According to visual observations, after a few seconds of cathodic polarization current, small gas bubbles appear on the aluminum electrode in Na_2MoO_4 (0.01 M) solution at a potential of -1.3 V, which accumulate on the electrode surface. As the cathode potential shifts to the negative side to -1.4 and further, the rate of the bubble formation and their number increase. At $E_{c,p} = -2.0$ V, the hydrogen evolution begins immediately and in large quantities when the cathodic polarization potential is switched on up to -3 V (Figs. 2 and 3). The currentless potential E (Fig. 4) significantly shifts to the negative side.

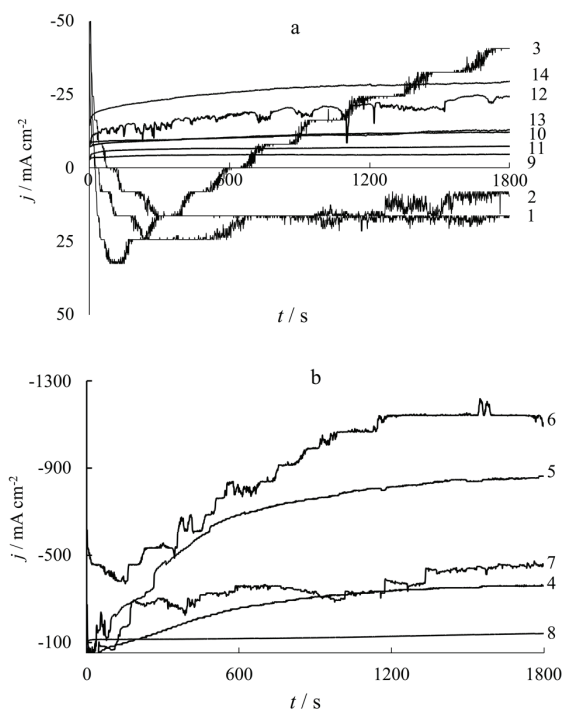


Fig. 2. Cathodic chronoamperograms of the Al cathode at potentials $-E_c / \text{V}$:
 1) 1; 2) 1.1; 3) 1.2; 4) 1.3; 5) 1.6; 6) 1.5; 7) 1.6; 8) 1.8; 9) 2; 10) 2.2; 11) 2.4; 12) 2.6; 13) 2.8;
 14) 3.0 in Na_2MoO_4 (0.01 M) solution for 30 min.

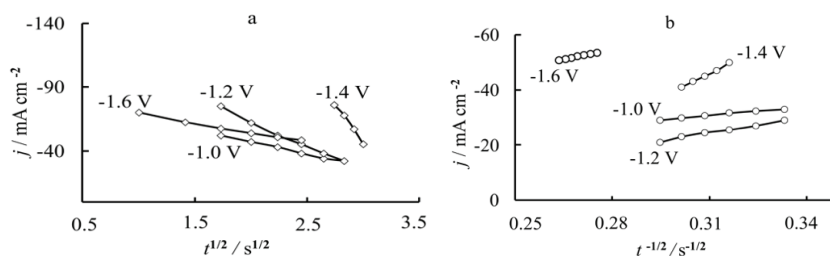


Fig. 3. Dependence a) $j-t^{1/2}$, b) $j-t^{-1/2}$ at the initial stage of the cathode polarization of Al in solution Na_2MoO_4 (0.01 M).

In the investigated potential range, two areas of current density can be distinguished (Fig. 2, curves 1–7 and curves 9–14) which differ in the mechanism of phase formation: the diffusion-kinetic mechanism of incorporation in the first case and the crystallization-chemical mechanism in the second one.^{5-7,9} It is important that in the first case the fixed value of the current density is 2 to 3 times higher than in the second one.

When H_3PO_4 (1 M) is added into Na_2MoO_4 (0.01 M) solution, the crystallization-chemical mechanism predominates on the Al electrode (Fig. 4) in the potential range from -1.0 to -2.0 V, both the electrode surface and the near-electrode layer of the solution turn blue.¹⁹ The analysis of the $j-t$ curves in the coordinates $j-t^{1/2}$ and $j-t^{-1/2}$ (Fig. 3) made it possible to calculate the diffusion-kinetic characteristics (Table I).^{29,35}

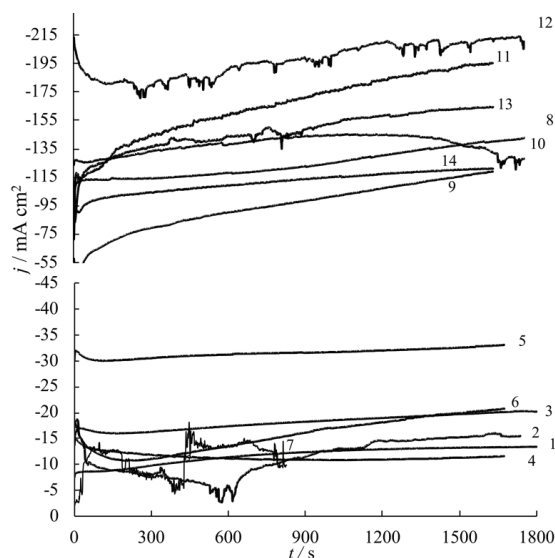


Fig. 4. Cathodic chronoamperograms of the Al cathode at potentials $-E_k$ / V: 1) 1; 2) 1.1; 3) 1.2; 4) 1.3; 5) 1.6; 6) 1.5; 7) 1.6; 8) 1.8; 9) 2; 10) 2.2; 11) 2.4; 12) 2.6; 13) 2.8; 14) 3.0 in solution: Na_2MoO_4 (0.01 M) + H_3PO_4 (1 M) for 30 min.

TABLE I. Influence of the potential of cathodic treatment on the diffusion-kinetic characteristics of the cathodic process at Al electrode in Na_2MoO_4 (0.01 mol)

E / mV	$j_{(t=0)}$ mA cm^{-2}	$K_{\text{p}}^{\text{I}} = \frac{\Delta i}{\Delta \sqrt{t}}$ $\text{mA} \cdot \text{cm}^{-2} \text{ s}^{-1/2}$	$K_{\text{p}}^{\text{II}} = \frac{\Delta i}{\Delta(1/\sqrt{t})}$ $\text{mA} \cdot \text{cm}^{-2} \text{ s}^{1/2}$	$C_0 D^{1/2}$ $\text{mol cm}^{-2} \text{ s}^{-1/2}$
-1	-42.8	22	100	0.002
-1.2	54	51	225	0.004
-1.4	60	222	100	0.009
-1.6	64	21	310	0.006
-2.2	7	1.4	0.2	$4.2 \cdot 10^{-6}$
-2.8	20	0.7	233	0.004

This discovered effect of the interface boundary $\text{Al}/\text{Na}_2\text{MoO}_4+\text{H}_3\text{PO}_4$ was explained by the molybdate ions property (nature): the molybdate ions pronounced ability increases with their polycondensation in the acidic medium. In the structure of heteropolyanions $[\text{PMo}_{12}\text{O}_{40}]^{3-}$ formed in the case of molybdenum, phosphorus is located in the center of a tetrahedron surrounded by 12 octahedrons, arranged in 4 groups containing three octahedra, in which each phosphorus atom has 4 oxygen atoms common to 3 octahedrons (MoO_6), 24 oxygen atoms in polyanion common to 2 octahedra (MoO_6) and 12 atoms are not bonded to others.

In the structures of heteropolyanions $[\text{PMo}_{12}\text{O}_{40}]^{3-}$, $[\text{PMo}_{11}\text{O}_{39}]^{7-}$, $[\text{P}_2\text{Mo}_{18}\text{O}_{62}]^{6-}$, $[\text{P}_2\text{Mo}_{17}\text{O}_{61}]^{10-}$, $[\text{P}_2\text{Mo}_5\text{O}_{23}]^{6-}$, $[\text{HP}_2\text{Mo}_5\text{O}_{23}]^{5-}$ a phosphorus atom occupies a central place.

The currentless potential E (Fig. 5) shifts significantly to the negative side. Studies of the morphology of the surface layer (Fig. 6) have shown that with the addition of a film-forming substance, chitosan, into the solution (Na_2MoO_4 (0.01 M) + solution H_3PO_4 (1 M)), a film-forming effect characteristic of chitosan is clearly observed, which rises with an increase in the duration and potential

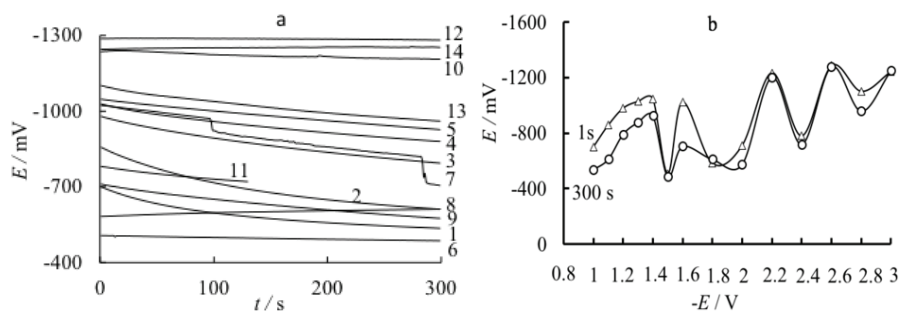


Fig. 5. The currentless potential ($E_{c/l}$, t) for the Al cathode; a) the dependence of $E_{c/l}$ on the E_{CP} ; b) for t of 1 and 300 s after cathodic polarization in the solution: Na_2MoO_4 (0.01 mol/l) at different potentials E_{c}/V : 1) -1.0; 2) -1.1; 3) -1.2; 4) -1.3; 5) -1.4; 6) -1.5; 7) -1.6; 8) -1.8; 9) -2; 10) -2.2; 11) -2.4; 12) -2.6; 13) -2.8; 14) -3.0.

of cathodic polarization, and the concentration of chitosan in the solution (Fig. 7). The catalytic effect of chitosan on the formation of a fiber structure precipitate is more clearly seen (Fig. 6, optical microscopy).

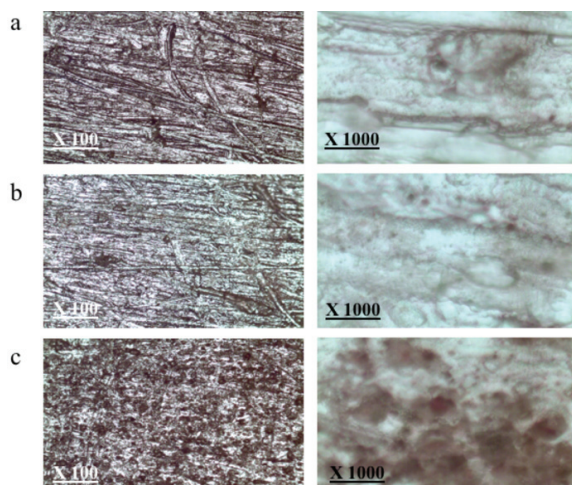


Fig. 6. Influence of the polarization duration on the morphology of the Al electrode surface in the electrolyte of the studied composition Na_2MoO_4 (0.01M) + H_3PO_4 (1 M) + chitosan (4 g/l; $t_{\text{grind}} = 60$ min) at $E_{\text{c,p}} = -2.6$ V and polarization time: a) 30; b) 45; c) 90 min.

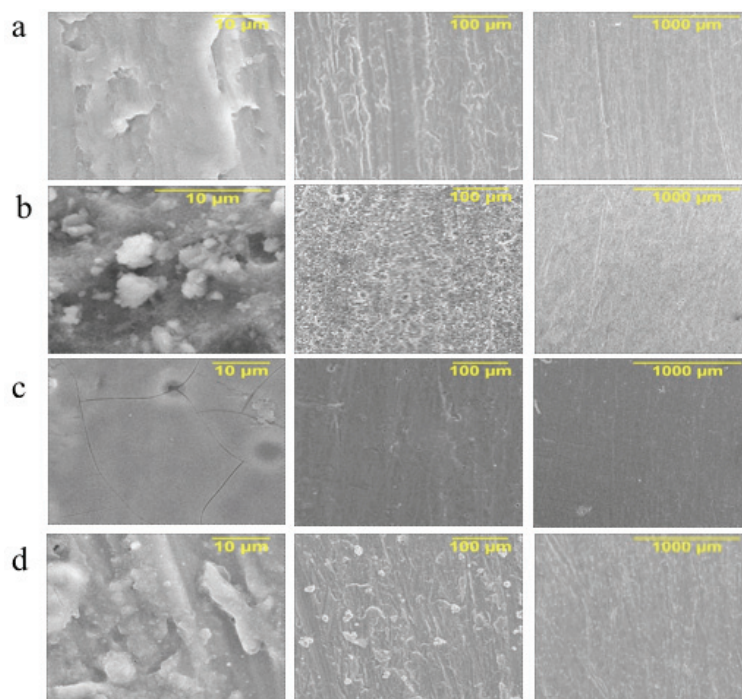


Fig. 7. Morphology of the Al electrode surface after cathodic treatment at $E_{\text{c}} = -2.6$ V and $t_{\text{cp}} = 90$ min in solutions: a) initial electrode, b) Na_2MoO_4 (0.01 M), c) Na_2MoO_4 (0.01 M) + H_3PO_4 (1 M) and d) Na_2MoO_4 (0.01 M) + H_3PO_4 (1 M) + chitosan (4 g/l, $t_{\text{grind}} = 60$ min).

The value of $E_{c/1}$ of the Al of electrode as before as after cathodic polarization shifts to the region of less negative values from -0.9 to -0.6 V at the first second (to the moment the electrode is immersed in the solution) and from -0.7 to -0.45 V after 300 s when the stationary state is established on the electrode (Fig 5b).

After cathodic treatment, depending on the value of the cathodic potential (-1.2 to -3.0 V), the electrode potential shifts significantly to the range of less negative values – at the time adding H_3PO_4 to Na_2MoO_4 solution (Table II). The H_3PO_4 addition shows structural action and as result, more aquability proportional change as before as after cathodic polarization at region E_c from -1.0 to -3.0 V.

TABLE II. Currentless potentials E/mV of the Al electrode after cathodic treatment at different potentials, depending on the composition of the solution at the first and 300th s after opening the circuit

Cathodic treatment potential, V	Na_2MoO_4 (0.01 M)		Na_2MoO_4 (0.01 M) + H_3PO_4 (1 M)		Na_2MoO_4 (0.01M) + H_3PO_4 (1 M) + chitosan (4 g/l; $t_{grind} = 60$ min)	
	at 1 s	at 300 s	at 1 s	at 300 s	at 1 s	at 300 s
-1.0	-699	-537	-626	-363		
-1.1	-856	-612	-642	-213		
-1.2	-978	-793	-614	-214		
-1.3	-1028	-879	-706	-212		
-1.4	-1047	-926	-647	-230		
-1.5	-507	-488	-759	-237		
-1.6	-1024	-705	-655	-227		
-1.8	-582	-612	-582	-238		
-2.0	-711	-576	-716	-202		
-2.2	-1235	-1205	-618	-225		
-2.4	-800	-720	-653	-218		
-2.6	-1286	-1281	-213	-151	-556	-232
-2.8	-1101	-959	-780	179		
-3.0	-1243	-1252	-726	-185		

The nature of the dependence of E on the value of the $E_{c,p}$ allows us to discuss about the formation of phases of variable composition, and about the accumulation of hydrogen and sodium in their composition as the $E_{c,p}$ shifts to the negative side.

As can be seen from Table III, with the higher duration of polarization, the amount of the oxide-containing phase in the surface layer increases. These can be aluminum oxides Al_2O_3 , Na_2O , nAl_2O_3 , (MoO_3) , MoO_4^{2-} , phosphates, phosphate derivatives of chitosan, embedded in a single heteropolymer fibrous-type structure, which is in good agreement with the results of the investigation of the morphology of the modified electrode surface (Figs. 6 and 7).

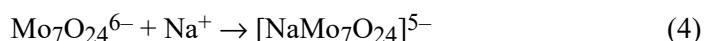
With the addition of chitosan additives (4 g/l) the solution becomes cloudy at the phase boundary and the precipitate of the forming phase becomes looser but retains its fibrous structure.

TABLE III. Elemental composition of the modified layer on the surface of the Al electrode after cathodic treatment in the solution Na_2MoO_4 (0,01 M) + H_3PO_4 (1 M) + chitosan (4 g/l; $t_{\text{grind}} = 60$ min) at $E_c = -2.6$ V and different polarization times ($t_{\text{cp}} / \text{min}$). Average values over 5 points; τ_p – polarization time

τ_p / min	Content, wt.%						
	C	O	Al	P	Mo	Na	Mn
30	28.56	49.29	14.0	6.8	1.2	0.08	0.03
60	18.6	42.8	20.5	11.4	6.3	0.24	0.33
90	4.0	50.84	17.0	13.9	4.25	0.27	0.01

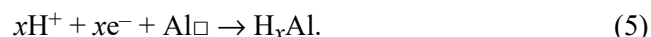
CONCLUSION

When adding phosphoric acid H_3PO_4 (1M) to the solution, the equilibrium of the reaction of the formation of polynuclear complexes:



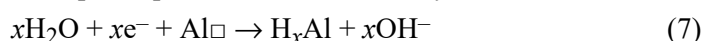
shifts strongly to the right and the concentration of mononuclear complexes MoO_4^{2-} , HMoO_4^- , H_2MoO_4 (respectively NaMoO_4^- and Na_2MoO_4) does not exceed 1–3 %. The protonated cations H_4PO_4^+ present in the solution are involved in the formation of polymeric heteronuclear formations with molybdate ions of the polyelectrolyte structure. Phosphate-molybdates of the alkali metal in the crystalline state are substitutional solid solutions $\text{Na}_{1-y}\text{Ti}_2(\text{MoO}_4)_y(\text{PO}_4)_{3-y}$ in the range $0 \leq y \leq 0.6$. The introduction of chitosan (4 g/l) into the solution of Na_2MoO_4 and H_3PO_4 is accompanied by a sharp increase in the film-forming effect.

Under the conditions of cathodic polarization, Na^+ accumulating near the electrode surface, under the action of a concentration gradient migrate through the layer of electrochemical adsorption products deep into the electrode and, at the boundary with metallic aluminum, participate in the formation of an interstitial phase according to the vacancy mechanism:



$\text{Al}\square$ – Al vacancy

At potentials more negative than -1 V in aqueous solutions, the formation of aluminum hydrides with the participation of H_2O or directly:



The existence of two potential regions, which are established, confirms the occurrence of two different processes with the participation of the $[\text{NaMo}_7\text{O}_{24}]^{5-}$ polynuclear complexes on the electrode in the adsorbed layer. The product of surface adsorption of polynuclear complexes could be double salts such as $\text{Na}_6\text{Al}_n\text{Mo}_{7-n}\text{O}_{24}$ and $\text{Na}_{1-y}\text{Al}_2(\text{MoO}_4)_y(\text{PO}_4)_{3-y}$ which have the properties of substitutional solid solutions.

ИЗВОД

ЕЛЕКТРОХЕМИЈСКО ФОРМИРАЊЕ ЈОНСКИ ПРОВОДНОГ ПОЛИМЕРА
ОКСО-ФОСФАТ-МОЛИБДАТА НА АЛУМИНИЈУМУ

HUSSEIN HUSSEIN¹, SWETLANA POPOVA², IRINA FROLOVA² и MARINA LOPUKHOVA²

¹Department of Chemistry and Chemical Technology of Materials, Yuri Gagarin State Technical University of Saratov, Saratov, Russia и ²Engels Technological Institute (branch) of Yu. Gagarin Saratov State Technical University, Engels, Russia

Електрохемијско понашање алуминијумске електроде у воденом раствору који је садржао Na_2MoO_4 , H_3PO_4 и хитосан је испитивано методама хронопотенциометрије на отвореном колу, хроноамперометрије, оптичке и скенирајуће електронске микроскопије. Модификација површине полимолибдат-фосфат слојева је извршена у потенциостатском режиму на потенцијалима између -1 и -3 V током различитих времена поларизације (од 15 до 90 min). Одређиван је елементарни састав површинског слоја метала пре и после катодне поларизације. Утврђено је да је електрохемијски формирана полимерна матрична структура од јонски проводних (H^+ , Na^+) хетеронуклеарних полимолибдата и полифосфат-молибдатних комплекса двоструких соли $\text{Na}_6\text{Al}_n\text{Mo}_{7-n}\text{O}_{24}$ и $\text{Na}_{2y}\text{Al}_2(\text{MoO}_4)_y(\text{PO}_4)_{3-y}$. Брзина интеркалације водоника и натријума у структуру полиоксо-фосфатно-молибдатних слојева нагло расте са повећањем негативне вредности потенцијала. Додатак хитосана у раствор поспешује ефекат формирања филма на површини јонски проводног оксо-фосфат-молибдатног полимерног слоја.

(Примљено 13. септембра, ревидирано 27. новембра, прихваћено 8. децембра 2020)

REFERENCES

1. B. P. Tarasov, M. V. Lototskii, V. A. Yartys, *Russ. J. Gen. Chem.* **77** (2007) 694 (<https://dx.doi.org/10.1134/s1070363207040329>)
2. V. N. Ageev, I. N. Beckman, O. P. Burmistrova, *Interaction of Hydrogen with Metals*, Nauka, Moscow, 1987, p. 296 (<https://b-ok.cc/ireader/3065144>)
3. W. X. Chen, *Int. J. Hydrogen Energy* **26** (2001) 603 ([https://doi.org/10.1016/S0360-3199\(00\)00119-1](https://doi.org/10.1016/S0360-3199(00)00119-1))
4. K. Young, J. Nei, *Materials* **6** (2013) 4574 (<https://doi.org/10.3390/ma6104574>)
5. S. S. Popova, L. A. Alekseeva, B. N. Kabanov, *Russ. J. Electrochem.* **22** (1986) 1427
6. S. S. Popova, N. A. Sobgaida, *Izv. Vyssh. Uchebn. Zaved. Khim. Khim. Tekhnol.* **45** (2002) 84
7. N. G. Krapivny, *Russ. J. Electrochem.* **17** (1981) 678
8. W. X. Chen, *Intern. J. Hydrogen Energy* **26** (2006) 603 ([https://doi.org/10.1016/S0360-3199\(00\)00119-1](https://doi.org/10.1016/S0360-3199(00)00119-1))
9. A. V. Zvyaginiceva, *ISJAE* **21** (2015) 145 (<https://doi.org/10.15518/isjaee.2015.21.018>)
10. E. O. Chudotvorova, P. I. Bestuzhev, V. V. Kozlyakov, in *Proceedings of The III International Scientific and Practical Conference*, Minsk, 2016, Belarus, Collection of Abstracts, 2016, p. 43

11. A. V. Reznichenko, V. V. Rybalchenko, F. Z. Badaev, S. G. Ponomarev, A. A. Vasin, *J Chem. Eng. Process. Technol.* **8** (2017) 347(<https://doi.org/10.4172/2157-7048.1000347>)
12. Z. Ragaiy, L. Brenda, G. Diaz, C. S. Fewox, C. Ashley, J. Stowe, R. G. Gray, G. H. Andrew, *Chem. Comm.* **25** (2009) 3717 (<https://doi.org/10.1039/B901878F>)
13. C. C. Wang, Y. C. Chou, C. Y. Yen, *Procedia Eng.* **36** (2012) 105 (<https://doi.org/10.1016/j.proeng.2012.03.017>)
14. H. Z. Wang, D. Y. C. Zeung, M. K. H., M. Ni, *Renew. Sustain. Energy Rev.* **13** (2009) 845 (<https://doi.org/10.1016/j.rser.2008.02.009>)
15. H. Zou, S. Chen, Z. Zhao, W. Lin, *J. Alloys Compd.* **578** (2013) 380 (<https://doi.org/10.1016/j.jallcom.2013.06.016>)
16. R. Ripan, I. Chetyanu, *Inorganic chemistry. Vol. 2. Chemistry of Metals*, M publishing house Mir, Moscow, 1972, p.872
17. I. O. Grigorieva, A. F. Dresvyannikov, A. S. Zifirov, *Bullet. Kazan Tech. Univ.* **16** (2013) 271
18. A. Mueller, S. Roy, *Usp. Khim.* **71** (2002) 1101 (<https://doi.org/10.1070/rc2002v071n12abeh000751>)
19. N. A. Perekhrest, K. N. Pimenova, V. D. Litovchenko, *J. Appl. Chem.* **65** (1992) 1163
20. O. A. Stadnik, N. D. Ivanova, E. I. Boldyrev, L. I. Zheleznova, *Ukr. Chem. J.* **74** (2009) 55
21. E. E. Tekutskaya, I. Ya. Turyan, V. I. Kravtsov, V. V. Kondrat'ev, *Russ. J. Electrochem.* **27** (1991) 407
22. E. E. Tekutskaya, V. I. Kravtsov, *Ind. Lab. Diagn. Mater.* **64** (1998) 8
23. M. A. Krayukhina, N. A. Samoilova, I. A. Yamskov, *Usp. Khim.* **77** (2008) 854 (<https://doi.org/10.1070/RC2008v077n09ABEH003750>)
24. Ya. A. Kamenchuk, E. A. Zelichenko, V. V. Guzeev, *Perspektivnye materialy* **6** (2009) 66
25. V. Scheveleva, L. A. Zemskova, A. V. Voight, V. G. Kuryavy, *Khimicheskie Volokna* **2** (2008) 44
26. T. S. Khakamov, D. V. Feoktistov, L. A. Badykova, P. G. Kornilaev, R. R. Shavaleev, R. K. Mudarisova, *Russ. J. Appl. Chem.* **86** (2013) 1417 (<https://doi.org/10.1134/S1070427213090175>)
27. S. S. Popova, O. G. Kovalenko, V. V. Kurchavova, K. A. Belousov, *Perspektivnye materialy* **11** (2013) 35
28. S. S. Popova, H. A. Hussein, I. I. Frolova, V. F. Abdullin, *Electrochem. Energetic* **20** (2020) 99 (<https://doi.org/10.18500/1608-4039-2020-20-2-99-111>)
29. S. S. Popova, *Methods of investigation of kinetics of electrochemical processes*, Saratov State Technical University, Saratov, 2008, p.106
30. O. N. Lyubiev, *Numerical methods in electrochemistry*, NPI Publishing House, Novocheerkassk, 1982, p.68
31. V. L. Mironov, *Fundamentals of scanning probe microscopy: Textbook for senior students of higher educational institutions*, Institute for Physics of Microstructures of the Russian Academy of Sciences, Nizhny Novgorod, 2004, p. 110
32. V. M. Zolotarev, N. V. Nikonov, A. I. Ignatiev, *Modern methods for the study of optical materials Part 2*, ITMO University, St. Petersburg, 2013, p.166
33. J. I. Goldstein, H. Yahowitz, D. E. Newbury, E. Lilshin, J. W. Colby, J. R. Coleman, *Practical Scanning Electron Microscopy: Electron and Ion Microprobe Analysis*, Plenum Press, New-York, 1975, p.598 (<https://doi.org/10.1007/978-1-4613-4422-3>)
34. L. V. Baranova, E. L. Demina, *Metallographic etching of metals and alloys: Handbook*, Metallurgy, Moscow, 1968, p. 256
35. S. P. Chizhik, L. K. Grigorieva, R. N. Kuklin, *Doklady Akad. Nauk SSSR* **321** (1991) 1221.